DTU Library

Improving CryoSat-2 SARIn L1b Products to Account for Inaccurate Phase Difference: Impact on Sea Ice Freeboard Retrieval

Di Bella, Alessandro; Scagliola, Michele ; Maestri, Luca; Skourup, Henriette; Forsberg, René

Published in:
I E E E Geoscience and Remote Sensing Letters

Link to article, DOI:
10.1109/LGRS.2019.2919946

Publication date:
2020

Document Version
Peer reviewed version

Citation (APA):
Di Bella, A., Scagliola, M., Maestri, L., Skourup, H., & Forsberg, R. (2020). Improving CryoSat-2 SARIn L1b Products to Account for Inaccurate Phase Difference: Impact on Sea Ice Freeboard Retrieval. *I E E E Geoscience and Remote Sensing Letters*, *17*(2), 252 - 256. https://doi.org/10.1109/LGRS.2019.2919946

Improving CryoSat-2 SARIn L1b products to account for inaccurate phase difference: impact on sea ice freeboard retrieval

Alessandro Di Bella, Michele Scagliola, Luca Maestri, Henriette Skourup, and René Forsberg

***Abstract*—CryoSat-2 is the first mission carrying on board an altimeter instrument able to operate in Synthetic Aperture Radar Interferometric (SARIn) mode. CryoSat-2 SARIn acquisitions have been exploited for different scientific applications that take advantage of the capability to determine the across-track angle of the first return and in particular they have been proved to reduce the uncertainty of sea ice freeboard retrievals. Nonetheless, the analysis of pan-Arctic freeboard obtained by processing CryoSat-2 Baseline C L1b products has shown large negative freeboard estimates in correspondence of the beginning of SARIn acquisitions. Throughout the paper, the SARIn waveforms are analysed to identify the cause of this behaviour. An improvement of the CryoSat-2 L1b processor is then prototyped and used to obtain a pan-Arctic freeboard dataset where the percentage of negative freeboard is successfully minimized.**

***Index Terms*—CryoSat-2, SARIn, altimetry, interferometry, sea ice freeboard.**

I. INTRODUCTION

THe primary goals of the ESA's Earth Explorer CryoSat-2 (CS2), launched on the 8th of April 2010, are the precise monitoring of the changes in the thickness of marine ice floating in the polar oceans and of the variations in the thickness of vast ice sheets [1]. The main payload of CS2 is a Ku-band pulse-width limited radar altimeter, called SIRAL (SAR Interferometric Radar ALtimeter), that is equipped with two antennas for single-pass interferometric capability. SIRAL can operate in three scientific measurement modes: Low Resolution Mode (LRM), Synthetic Aperture Radar (SAR) mode and SAR-Interferometric (SARIn) mode. In SAR/SARIn modes, exploiting the coherence of the emitted pulses, the along-track resolution is improved performing Delay/Doppler processing on ground [2].

The purpose of the CS2 interferometer is to determine the across-track location of the received echo. When operating in SARIn mode, SAR processing is combined with across-track interferometry exploiting the echoes received by a second across-track antenna. The complex conjugate cross product of the echoes received by both antennas is formed, and the argument is the phase difference between the two echoes resulting from the different distance travelled to reach the two antennas. Across-track interferometry allows SIRAL to determine the angle to the point of closest approach (POCA) [3]. CS2 was equipped with this capability to improve the performance of the altimeter over that of pulse limited radars when operating over surfaces with complex topography.

A. Di Bella, H. Skourup and R. Forsberg are with DTU Space, National Space Institute, Technical University of Denmark, Elektrovej 327, Kgs. Lyngby, Denmark (email: adia@space.dtu.dk; hsk@space.dtu.dk; rf@space.dtu.dk)

M. Scagliola and L. Maestri are with Aresys, via Privata Flumendosa 16, Milan, Italy (e-mail: michele.scagliola@aresys.it; luca.maestri@aresys.it).

This work was partially supported by the European Space Agency under Contract No. 4000111474/14/I/NB.

The analysis of CS2 SARIn acquisitions was exploited to track changes in the elevation and mass of the polar ice sheets [1], which was one of the primary objective of the mission. Additionally, novel scientific applications of SARIn data have been studied, such as inland water monitoring, coastal zone altimetry and swath mode processing [1]. Among them, different studies have shown that a reduced uncertainty in the freeboard heights can be obtained exploiting the interferometric information [4], [5]. Despite the overall improvement on the freeboard accuracy by including the interferometric information in the processing, discontinuous freeboard heights were retrieved at the boundary of the SARIn patches, as discussed in Sect. II. Those results were obtained by processing CS2 SARIn Level 1b (L1b) from the version C of the products, that are obtained from the current version of the ESA processor chain. This paper is aimed at analysing the cause of these discontinuities and at demonstrating that the accuracy of the phase difference in CS2 SARIn L1b products can be increased by improving the current version of the CS2 SAR/SARIn Level 1 Instrument Processing Facility (IPF1), that is the processor in charge of generating the L1b products.

II. FREEBOARD RETRIEVAL FROM CRYOSAT-2 SARIN ACQUISITIONS

Sea ice freeboard is referred to as the height of the sea ice above the local sea surface. For the last 25 years satellite altimetry has proven to be a powerful tool to measure sea ice freeboard and, thus, to estimate sea ice thickness. Freeboard can be measured using satellite altimetry by discriminating between echoes coming from sea ice and those coming from leads [6]—fractures in the sea ice cover caused by diverging ice motion and representing the local sea surface height. The very different roughness of these two surfaces determines the shape of the radar altimetry waveforms. Waveforms generating from leads, quasi-specular surfaces, resemble the impulse response of SIRAL [7], i.e., they are very "peaky" and have a very large power compared to sea ice waveforms, characterized by a more diffusive look.

One of the challenges when measuring freeboard with satellite altimetry is the accurate estimation of the sea surface

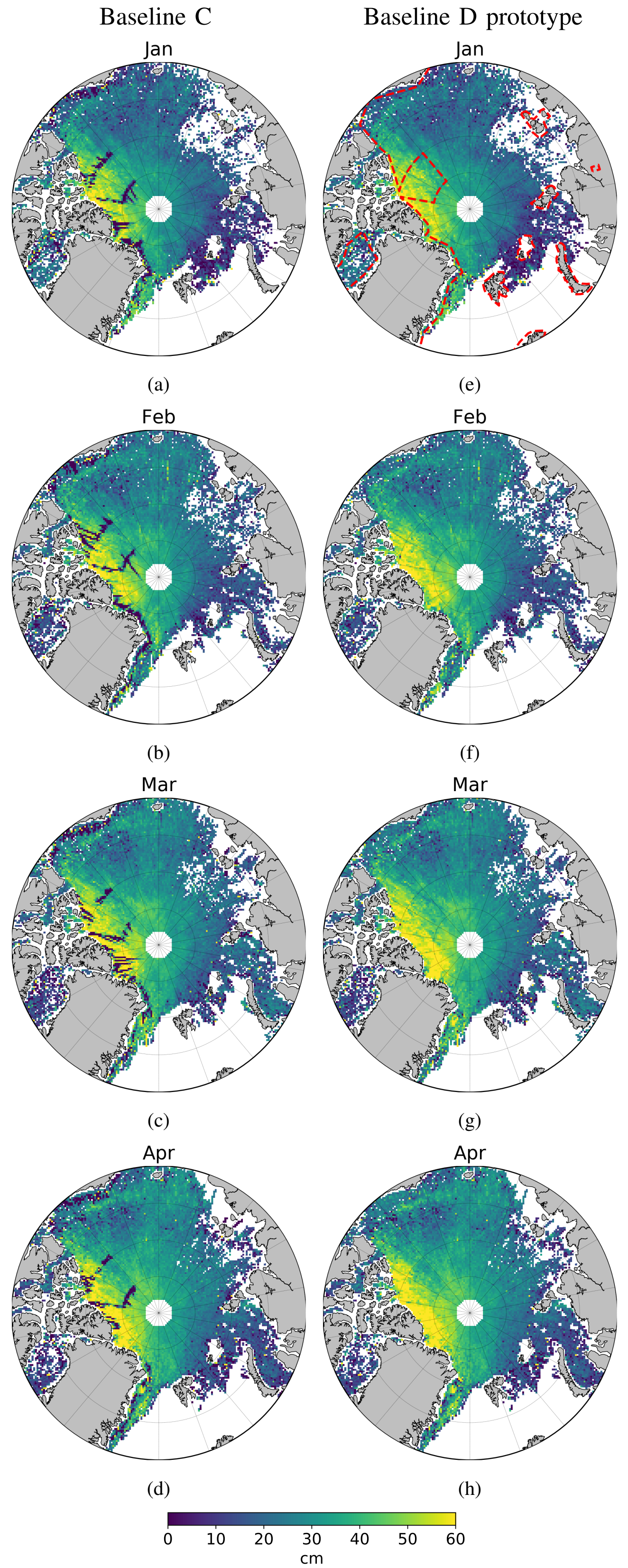

Fig. 1. Gridded monthly freeboard from Baseline C (a-d) and Baseline D prototype (e-h) L1b data for the period Jan–Apr 2014. The dashed red line in (e) represents the boundaries of the SARIn acquisition mask

height (SSH) in sea ice covered areas. The uncertainty of the SSH throughout the Arctic Ocean highly depends on the amount of leads detected by the satellite as well as by their spatial distribution. Echoes generated by off-nadir leads can dominate the satellite waveform [8] ultimately causing, if not accounted for, an underestimation of the SSH, as shown by [4]. The same study additionally shows that the phase information available in the SARIn acquisition mode can be used to estimate the across-track location of leads, correct for the range overestimation and ultimately get a more precise value of the along-track SSH. The higher precision of the SSH enables, in turn, to reduce the uncertainty of the sea ice freeboard retrievals, as shown by [5].

This study uses CS2 L1b SAR and SARIn waveforms from the latest Baseline C products. While it has been shown by [9] that the maximum power of the waveform is likely the most significant parameter aiding lead detection, surface classification is performed here using the "pulse peakiness" of the waveform, as it enables to separate returns from off-nadir leads, sea ice and leads detected at nadir (purely specular echoes) [4], [5]. All waveforms are retracked using a TFMRA50% threshold retracker based on the one recommended by [10] and the surface heights obtained from SARIn waveforms are corrected applying the off-nadir range correction (ONC) [4], [5]. All elevations are detrended using the DTU15 mean sea surface to improve the accuracy of the interpolated SSH. The local sea surface anomaly is then obtained by along-track linear interpolation of the lead heights, smoothed using a 25-km moving window to account for the noise of individual lead elevations [10]. Finally, freeboard heights are retrieved by subtracting the local sea surface anomaly from the sea ice elevations. A snow range correction accounting for the lower wave propagation speed into snow is applied according to [5], using snow depths and densities from the modified Warren 99 climatology [11], [12] and ice types from the "Sea ice type product of the EUMETSAT Ocean and Sea Ice Satellite Application Facility" (OSI SAF, www.osi-saf.org). For a more detailed description of the processing steps, the reader is referred to [5].

Fig. 1a-1d show the gridded monthly freeboard in the Arctic Ocean from Baseline C L1b data for the period Jan–Apr 2014. White areas in the plots represent both areas where no sea ice is present—east of Greenland and south of Svalbard—as well as areas where waveforms are discarded by the processor e.g. because of the lack of detected leads or other processing errors. The freeboard spatial distribution shows the similar large-scale patterns that have been observed throughout the years from different satellite sensors, e.g. [6], [13], [12], [14], with the thicker ice growing off the northern coast of Greenland and Canada thinning when moving towards the central Arctic. The most prominent feature in Fig. 1a-1d, however, is the negative value of freeboard at the boundaries of the SARIn acquisition mask (dashed red line in Fig. 1e). This is attributed to overestimated values of SSH from SARIn data. The fact that the SSH is interpolated and filtered along the satellite track [5] explains the smearing effect of the negative freeboard. As shown in Fig. 2, the negative freeboard values disappear when the ONC is not applied. Further analysis confirmed that the

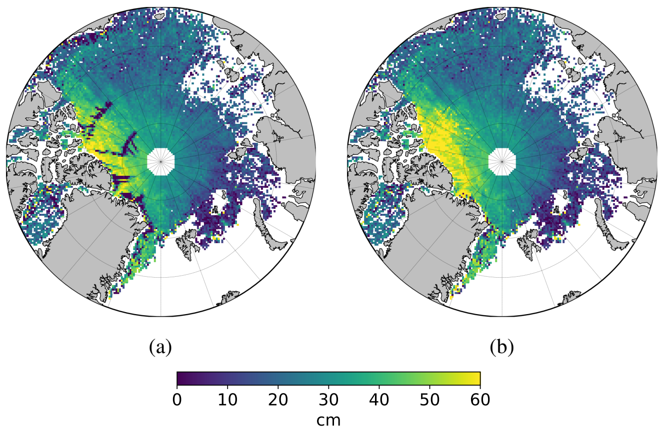

Fig. 2. Gridded freeboard from Baseline C L1b data for Jan 2014, with (a) and without (b) the ONC applied to the SARIn range measurements

overestimated SSH are indeed caused by large values of ONC used to correct the SARIn range measurements.

Next section further investigates the accuracy of the phase difference between the echoes received at the two antennas, as this indirectly determines the value of ONC [4]. The negative freeboard pattern in Fig. 1a-1d has not been observed before, probably because the majority of the current freeboard processors treat SARIn waveforms as degraded, i.e. noisier, SAR waveforms, discarding the phase information. Also, large negative values of freeboard are usually flagged as erroneous by most processing chains and automatically discarded.

III. Improving phase difference in CryoSat-2 SARIn L1b products

A detailed analysis of CS2 Baseline C SARIn L1B products was performed, aiming at investigating the behaviour described in Sect. II. Such analysis was focussed on the phase difference and the coherence of the waveforms in correspondence of the retracking point. Fig. 3 shows the phase difference and the coherence at the retracking point for the first 210 waveforms in a Baseline C SARIn L1b product where SIRAL just switched to SARIn mode. Even if the results in Fig. 3 have been obtained identifying the retracking point with an OCOG retracker with threshold 0.8, the phase difference evolution as function of the waveform does not depend on the retracker adopted. There it can be observed that the phase difference of the first waveforms is much higher than in the rest of the product and that the corresponding coherence is low. Those results suggested that the artefacts discussed in Sect. II were likely to be addressed to inaccurate values of phase difference for the first ∼40 waveforms in Baseline C SARIn L1b products.

Further analysis revealed that the current version of the CS2 SAR/SARIn IPF1 does not apply an instrument-related phase difference correction, namely CAL4, to the first 19 bursts of each acquisition. This is due to the fact that the first CAL4 burst is retrieved about 1 second after the first science burst. It is worth recalling that the CAL4 correction aims to calibrate the phase difference between the two receiving chains [15]. CAL4 calibration is interleaved in the SARIn measurements and it is performed with a repetition frequency of 1 Hz. It has to be underlined that since each science burst contributes to several waveforms, the inaccurate phase difference in the first 19 bursts affects roughly the first 40 waveforms of each SARIn L1b product, as shown in Fig. 3.

A prototype version of the CS2 SAR/SARIn IPF1 was implemented in order to apply the closest in time CAL4 correction to the first 19 bursts of each acquisition. The obtained improvement on the phase difference and on the coherence at the retracking point can be noticed in Fig. 3. The phase difference of the first waveforms is aligned to the phase difference of the following ones and the corresponding coherence is high. The next version of the CS2 SAR/SARIn IPF1, that will be used to generate the Baseline D L1b products, is planned to include this functionality in order to improve the quality of the phase difference information.

IV. Results

In order to assess the impact of the improvements described in Sec. III on the estimated freeboard, the Baseline D prototype L1b processor was used to regenerate the L1b SARIn products for the period Jan–Apr 2014. Fig. 1e-1h show the gridded

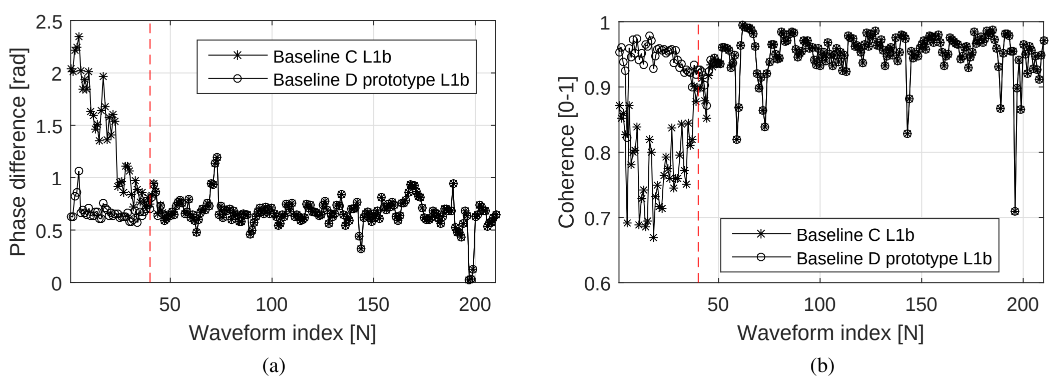

Fig. 3. Phase difference (a) and coherence (b) at the retracking point for the first 210 waveforms in the product CS_OFFL_SIR_SIN_1B_20180125T012006_20180125T012109_C001.DBL. The dashed red line is drawn in correspondence of the 40th waveform

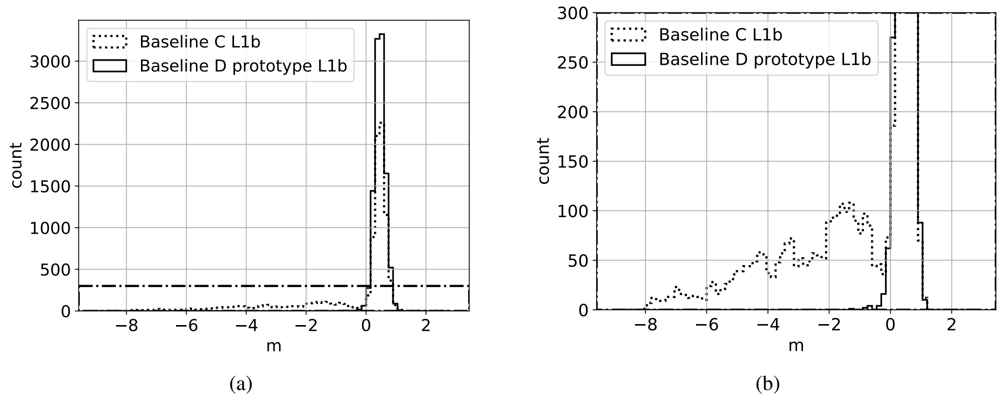

Fig. 4. Freeboard distribution within the area of interest (Sect. IV) from Baseline C (dotted) and Baseline D prototype (solid) data for January 2014. The rectangle at the bottom of (a) is enlarged in (b). The total number of freeboard retrievals is $\sim$10000

monthly freeboard from the new data. Comparing these results with those from Baseline C in Fig. 1a-1d, one can observe that the artificial pattern along the boundaries of the SARIn acquisition mask has disappeared, highlighting a continuous freeboard spatial distribution throughout the Arctic.

To get a more quantitative picture of the improvements achieved by the Baseline D prototype, the freeboard distribution within a 12-km area around the northern, eastern and southern boundaries of the Wingham box—the SARIn patch in the Canadian Arctic in Fig. 1e—is computed for January 2014. The distributions for Baseline C and Baseline D prototype are compared in Fig. 4. The western boundary is not included in the histograms since here SIRAL, due to the CS2 orbit inclination, does not switch from LRM/SAR to SARIn, but only from SARIn to LRM/SAR modes—which is the reason why the western boundary is not affected by the issue in Fig. 1a-1d. The distance of 12 km from the SARIn boundaries is chosen as this is approximately the maximum along-track distance on the ground covered by 40 20Hz CS2 waveforms (Sect. III). Within the area of interest, the freeboard estimated from Baseline C is largely negative with values down to -8 m (Fig. 4b). In Table I it can be noticed that the amount of negative freeboard estimates is reduced from 25.8% in Baseline C to 0.8% using the developed Baseline D prototype, with the remaining negative freeboard estimates mainly due to measurement noise. The improvement is also noticed on the mean value of freeboard inside the area of interest which increases from -37 cm to 46 cm (Table I), a more reasonable estimate for regions with predominantly thick multi-year sea ice [7].

TABLE I
BASELINE C VS. BASELINE D PROTOTYPE MEAN FREEBOARD (μ_F) AND PERCENTAGE OF NEGATIVE FREEBOARD ESTIMATES (F_n) INSIDE THE AREA OF INTEREST (SECT. IV) FOR JANUARY 2014

	Baseline C	**Baseline D**
$\mu_\mathbf{F}$	-37 cm	46 cm
$\mathbf{F_n}$	25.8%	0.8%

The next Baseline for CS2 L1b products, i.e. Baseline D, will be corrected for the issues discussed in Sect. II and will deliver accurate values of freeboard also in areas where the instrument switches to SARIn mode. By increasing the amount of usable phase information, it will additionally contribute to reduce the freeboard uncertainty [5].

V. CONCLUSION

CS2 SARIn data have been used to successfully monitor changes in the elevation of ice sheets, as well as inland water and coastal areas. Recently, it has been shown that the phase information available in this acquisition mode can be used to reduce the uncertainty affecting sea ice freeboard retrievals [5].

Nevertheless, processing pan-Arctic Baseline C SARIn L1b products, exploiting the phase information, has shown large negative freeboard estimates at the boundary of the SARIn acquisition mask (Fig. 1a-1d). This issue, caused by a phase difference calibration not applied to the first 19 bursts of a SARIn acquisition, affects the quality of the phase information of the first $\sim$40 SARIn waveforms. By updating the current CS2 SAR/SARIn IPF1 to correctly apply such calibration (Sect. III), the quality of the freeboard at the SARIn boundaries improves drastically as the amount of negative retrievals is reduced from 25.8% to 0.8% (Table I). The pattern of negative freeboard observed, using Baseline C products, at the SARIn patch boundaries throughout the Arctic basin consequently disappears (Fig. 1e-1h).

This update will be included in the new CS2 SAR/SARIn IPF1 producing the upcoming Baseline D L1b products. Improvements are expected not only for sea ice freeboard retrieval, but for any application that exploits the phase information from SARIn L1b products. According to Sect. III, improvements will be observed in areas up to $\sim$12 km inside the SARIn acquisition mask. The improvement for inland water monitoring applications will be significant especially w.r.t. monitoring small water bodies and narrow rivers, where discarding the first 19 to 40 waveforms might not always be a viable option.

ACKNOWLEDGEMENTS

The CryoSat-2 data are provided by the European Space Agency and the sea ice type products are produced by the

EUMETSAT Ocean and Sea Ice Satellite Application Facility (OSI SAF, www.osi-saf.org).

REFERENCES

[1] T. Parrinello, A. Shepherd, J. Bouffard, S. Badessi, T. Casal, M. Davidson, M. Fornari, E. Maestroni, and M. Scagliola, “CryoSat: ESA’s ice mission – Eight years in space,” *Advances in Space Research*, vol. 62, no. 6, pp. 1178 – 1190, 2018, the CryoSat Satellite Altimetry Mission: Eight Years of Scientific Exploitation.

[2] R. Raney, “The delay/doppler radar altimeter,” *Geoscience and Remote Sensing, IEEE Transactions on*, vol. 36, no. 5, pp. 1578–1588, Sep 1998.

[3] D. Wingham, L. Phalippou, C. Mavrocordatos, and D. Wallis, “The mean echo and echo cross product from a beamforming interferometric altimeter and their application to elevation measurement,” *Geoscience and Remote Sensing, IEEE Transactions on*, vol. 42, no. 10, pp. 2305–2323, Oct 2004.

[4] T. W. K. Armitage and M. W. J. Davidson, “Using the Interferometric Capabilities of the ESA CryoSat-2 Mission to Improve the Accuracy of Sea Ice Freeboard Retrievals,” *Ieee Transactions on Geoscience and Remote Sensing*, vol. 52, no. 1, pp. 529–536, 2014.

[5] A. Di Bella, H. Skourup, J. Bouffard, and T. Parrinello, “Uncertainty reduction of Arctic sea ice freeboard from CryoSat-2 interferometric mode,” *Advances in Space Research*, vol. 62, no. 6, pp. 1251 – 1264, 2018, the CryoSat Satellite Altimetry Mission: Eight Years of Scientific Exploitation.

[6] S. Laxon, N. Peacock, and D. Smith, “High interannual variability of sea ice thickness in the Arctic region,” *Nature*, vol. 425, no. 6961, pp. 947–950, 2003.

[7] R. Kwok and G. F. Cunningham, “Variability of Arctic sea ice thickness and volume from CryoSat-2,” *Philosophical Transactions of the Royal Society of London A: Mathematical, Physical and Engineering Sciences*, vol. 373, no. 2045, p. 20140157, 2015.

[8] M. R. Drinkwater, “K_u band airborne radar altimeter observations of marginal sea ice during the 1984 Marginal Ice Zone Experiment,” *Journal of Geophysical Research*, vol. 96, no. C3, pp. 4555–4572, 1991.

[9] A. Wernecke and L. Kaleschke, “Lead detection in Arctic sea ice from CryoSat-2: Quality assessment, lead area fraction and width distribution,” *Cryosphere*, vol. 9, no. 5, pp. 1955–1968, 2015.

[10] R. Ricker, S. Hendricks, V. Helm, H. Skourup, and M. Davidson, “Sensitivity of CryoSat-2 Arctic sea-ice freeboard and thickness on radar-waveform interpretation,” *Cryosphere*, vol. 8, no. 4, pp. 1607–1622, 2014.

[11] S. Warren, I. Rigor, N. Untersteiner, V. Radionov, N. Bryazgin, Y. Aleksandrov, and R. Colony, “Snow depth on Arctic sea ice,” *Journal of Climate*, vol. 12, no. 6, pp. 1814–1829, 1999.

[12] S. W. Laxon, K. A. Giles, A. L. Ridout, D. J. Wingham, R. Willatt, R. Cullen, R. Kwok, A. Schweiger, J. Zhang, C. Haas, S. Hendricks, R. Krishfield, N. Kurtz, S. Farrell, and M. Davidson, “CryoSat-2 estimates of Arctic sea ice thickness and volume,” *Geophysical Research Letters*, vol. 40, no. 4, pp. 732–737, 2013.

[13] R. Kwok, G. F. Cunningham, M. Wensnahan, I. Rigor, H. J. Zwally, and D. Yi, “Thinning and volume loss of the Arctic Ocean sea ice cover: 2003–2008,” *Journal of Geophysical Research: Oceans (1978?2012)*, vol. 114, no. C7, 7 2009. [Online]. Available: http:https://doi.org/10.1029/2009JC005312

[14] T. W. K. Armitage and A. L. Ridout, “Arctic sea ice freeboard from AltiKa and comparison with CryoSat-2 and Operation IceBridge,” *Geophysical Research Letters*, vol. 42, no. 16, pp. 6724–6731, 2015.

[15] M. Fornari, M. Scagliola, N. Tagliani, T. Parrinello, and A. G. Mondejar, “CryoSat: SIRAL calibration and performance,” in *2014 IEEE Geoscience and Remote Sensing Symposium*, July 2014, pp. 702–705.